Proceedings of the 20th International Conference on Soil Mechanics and Geotechnical Engineering– Rahman and Jaksa (Eds)

Static tension load tests performed on resin grouted micropiles

Essais de chargement statique de traction sur des micropieux en résine

Nicolas Denies & Malek Allani
Geotechnical Division, Belgian Building Research Institute, Belgium, nicolas.denies@bbri.be

Noël Huybrechts
Geotechnical Division, Belgian Building Research Institute & KU Leuven, Belgium

Piet Kempenaers & Dominique Smits
GCP Applied Technologies, Belgium

ABSTRACT: An in-situ test campaign was performed in the facilities of the BBRI to study the geotechnical behavior of resin grouted micropiles, consisting of hollow steel anchor bars covered by hardened resin. After the installation of hollow steel bars into the ground by dry drilling, expanding and curing synthetic resins are injected, throughout the hollow steel bars and they penetrate, at several depths via openings, into the surrounding soil to form, after chemical reaction, hardened resin bodies around the steel bars. The purpose of the present experimental test campaign was to determine the geotechnical tensile resistances (i.e. the uplift resistances) of three isolated resin grouted micropiles. Static tension load tests were performed to analyze their load-displacement behavior and to determine their uplift resistance when subjected to tensile loads. Within the test campaign, three different types of resin grouted micropiles were studied. The present paper provides the details of the test procedure and the main results of the three static tension load tests, conducted according to the French standard NF P 94-150-2. For the three different resin grouted micropiles, critical creep loads varied between 140 and 200 kN and the tensile loads at failure reached values ranging between 175 and 215 kN.

RÉSUMÉ : Une campagne d'essai in situ a été réalisée au sein des installations du CSTC afin d'étudier le comportement géotechnique de micropieux en résine. Ces derniers consistent en des barres d'ancrage creuses, en acier, recouvertes d'une résine durcie. Ces barres d'acier sont initialement forées à sec dans le sol. Ensuite, des résines expansives et durcissantes sont injectées à travers les barres et pénètrent, à différentes profondeurs, dans le sol via des ouvertures réalisées dans les barres pour former, après réaction chimique, un manteau de résine durcie autour des barres en acier. L'objectif de la présente campagne expérimentale est de déterminer la résistance géotechnique en traction de trois micropieux en résine isolés. Des essais de chargement statique en traction ont été effectués pour analyser leur comportement « charge-déplacement » et pour déterminer leur résistance à l'arrachement lorsqu'ils sont mis en tension. Trois différents types de micropieux en résines ont été étudiés. Le présent article fournit les détails de la procédure suivie pour la réalisation des essais, conduits selon la NF P94-150-2, et les résultats principaux. Pour les trois différents micropieux en résine, les charges critiques de fluage variaient entre 140 et 200 kN et les charges de tractions à la rupture entre 175 et 215 kN.

KEYWORDS: micropiles, injection, resin, geotechnical tensile resistance, SLT

1 INTRODUCTION

In October 2017, the company GCP APPLIED TECHNOLOGIES has made an appeal to the Belgian Building Research Institute (BBRI) in order to organize and to perform a geotechnical testing campaign on innovative resin grouted micropiles installed on the test site of the BBRI in Limelette (Belgium). The purpose of the in-situ test campaign was to study the geotechnical behavior of resin grouted micropiles, consisting of hollow steel anchor bars covered by hardened resin.

After the installation of hollow steel bars into the ground by dry drilling, expanding and curing synthetic resins are injected, through the hollow steel bars and they penetrate, at several depths via openings, into the surrounding soil to form, after chemical reaction, hardened resin bodies around the steel bars.

These new grouting type micropiles can be used for ground improvement works or for stabilizing existing foundations by soil consolidation generally up to a depth of five meter. In the case of underpinning projects, the individual resin grouted micropiles and the existing foundation are then fastened together.

The yield load of the hollow steel bars used within the framework of this test campaign, the DE NEEF® AXI Anchor Bars, is equal to 228 kN. The length of the steel bars, installed on the test site of the BBRI, was equal to 5 m. The external diameter of the bars was equal to 32 mm and their area to 430 mm².

Within the framework of the present test campaign, three kinds of resin were studied:
- the resin DE NEEF® AXI G1 (resin + catalyst),
- the resin DE NEEF® AXI G3 (two-component resin),
- and the resin DE NEEF® AXI G4 (two-component resin).

The installation depth of the bars was equal to 4.5 m.

2 GEOTCHNICAL CONTEXT

Before the beginning of the test campaign, several types of soil, present on the test site of the BBRI in Limelette, were tested in the laboratory facilities of GCP APPLIED TECHNOLGIES in Belgium. On the basis of several lab tests, it was decided to install the resin grouted micropiles in an artificial testing well of 5.5 m deep, previously installed on the test site of the BBRI, and filled with Brusselian sand coming from the sand quarry of Mont-St-Guibert (Belgium) where it is extracted for its use in the construction industry.

The purpose of this choice was to assess the geotechnical behavior of the resin grouted micropiles in a soil consisting in a loose sandy layer of about 5 m deep.

More information about the geological background of the Brusselian sand can be found in Vanden Berghe (2001). The analysis performed on a sand sample taken in the well highlighted the fact that it is a poorly-graded medium sand (d_{50} around 0.35 mm and Cu of 1.58) characterized by irregular shaped grains with round or angular edges.

In order to fulfill the purposes of the test campaign, it was decided to install eight resin grouted micropiles in the artificial sand well of the BBRI facilities.

The distance between each resin grouted micropile is 2.2 m to avoid mutual influence of the static load test (SLT) on neighboring piles.

For the geomechanical characterization, eight variable energy lightweight dynamic cone penetrometer tests (also called PANDA® tests) and six electric cone penetrometer tests (CPT's) were performed.

Before installing the steel bars into the ground, eight PANDA® tests were executed in the axis of the eight future resin grouted micropiles. The PANDA® tests were executed according to the NF P 94-105 with a cone presenting a surface area of 2 cm². Figure 1 presents the results of the PANDA® tests.

The six CPT's were executed according to the ISSMGE TC16 procedure (1999) with an electrical cone of 10 cm². Figure 2 provides an oversight of the results of the six CPT's. The positions of the CPT's are indicated in the inset of Figure 2.

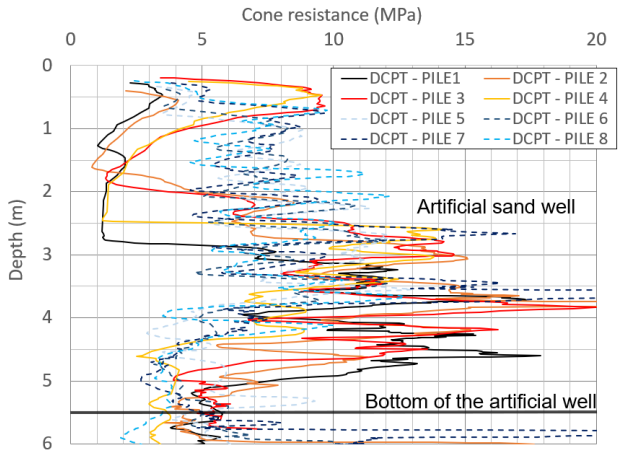

Figure 1. Results of the eight Panda® tests

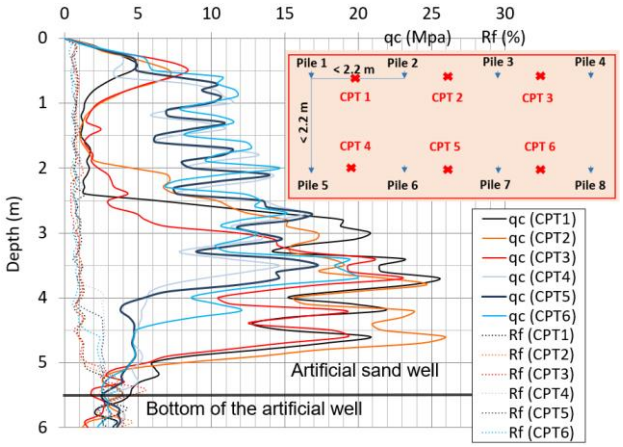

Figure 2. Results of the six CPT's with electrical cone

3 INSTRUMENTATION OF THE STEEL BARS WITH OPTICAL FIBERS

Before installation into the ground, the hollow steel bars were instrumented in the laboratory facilities of the BBRI. The instrumentation consisted in an optical fiber integrated into the body of the steel bar to follow the deformations of the steel material during the future SLT's.

The optical fiber technology used within the framework of the present test campaign is the Fiber Bragg Gratings technique (FBG). With that technology, a multitude of sensor points are available on one single optical fiber.

The working principle of the Fiber Bragg Gratings technology (FBG) is described in Huybrechts et al. (2016). One single continuous optical fiber is at several well-defined positions provided with a Bragg grating that serves as a sensor. At the position of such a Bragg grating an incident spectrum from a light source is reflected at a specific (predetermined) wavelength. By providing Bragg gratings at several positions on the optical fiber and at the condition that each Bragg grating reflects the incident spectrum at a different wavelength, a multi-point sensor can be obtained. With this technology, variations of parameters such as the temperature or the deformation at the location of the Bragg grating shift in a linear way the reflected wavelength, reason why this technology can be used as sensor device e.g. to measure the deformation at the location of the grating (Huybrechts et al., 2016).

For the present project, five sensing areas or sensors are provided on each continuous optical fiber. That means that, during the SLT's, the deformation of the steel bars will be measured at five different locations. The five locations of measurement have been defined as follows. The first sensor is installed 10 cm above the micropile base (= 10 cm above the underside of the steel bar to be installed into the ground). The spacing between all the sensors is 90 cm.

4 REALIZATION OF THE RESIN GROUTED MICROPILES

The eight DE NEEF® AXI anchor bars were first drilled into the ground with a dry process (see Figure 3). During the process, neither water, nor drilling grout/liquid were used.

Figure 3. Dry drilling of the steel bars into the ground

Five meter long steel bars were installed in one operation (installation depth of 4.5 m). No coupling sleeves were used. Just after installation of the steel bars into the ground, the staff of GCP APPLIED TECHNOLOGIES has cleaned and installed the injection tubes inside the hollow steel bars (see Figure 4).

After the installation of the steel bars into the ground, eight reinforced concrete slabs were installed around the bars in order to simulate the presence of a building slab at the surface of the soil (as for underpinning projects) and to provide the proper containment for the injection material.

For the purpose of isolating the steel bar from the concrete slab, at the level of the future concrete slab, the steel bar was covered with a classical PU foam injected inside a PVC tube (see Figure 5). During the SLT's, the concrete slabs were removed. Figure 6 presents the test location after concreting of the eight slabs.

Figure 4. Installation of the injection tube inside the hollow steel bar

Figure 5. Isolation of the steel bar with the PU foam

Figure 6. Test location after concreting the eight slabs

The injection process was performed one week after the installation of the concrete slabs. The micropiles ID 1, 2 and 5 were injected with the resin DE NEEF® AXI G1, the micropiles ID 3, 6 and 7 with the resin DE NEEF® AXI G4 and the micropiles ID 4 and 8 with the resin DE NEEF® AXI G3. Figure 7 illustrates the injection phase.

Figure 7. Injection phase

5 REALIZATION OF A FIRST IN-SITU TEST CAMPAIGN WITH STATIC COMPRESSION LOAD TESTS

Before the realization of the static tension load tests, six static compression load tests were performed according to the NF P 94-150-1 on six isolated resin grouted micropiles to analyze their load-settlement behavior and to determine their bearing capacity when subjected to compressive loads. This first test campaign with compression tests is reported and detailed in Denies et al. (2019). Main results are given in the following paragraphs.

During the first test campaign (i.e. the six SLT's in compression), the geotechnical bearing capacity of the resin grouted micropiles was never reached. Either a structural failure of the steel bar was observed (by buckling) or a high level of deformation was reached in the steel bar. That means that, in the given soil conditions, the bearing capacity of such micropiles is limited by the steel strength. The tests also demonstrated the effective geotechnical behavior of the resin body of the micropile with a significant level of friction mobilization at the interface resin-soil (see Denies et al. 2019).

A comparison of the load-settlement curves obtained for the six tested micropiles is given in Figure 8. Within the framework of this geotechnical test campaign, a sudden structural failure of the micropile by buckling of the steel bar was observed for the micropiles ID 2 (failure at 111 kN during the increase of the load), ID 7 (after 10 minutes of loading at 180 kN) and ID 8 (at 138 kN during the increase of the load). In Figure 8, the dotted lines indicate the last measurements taken just before failure.

A level of deformation close to the yield strength of the steel bar was observed for the micropiles ID 1 and 4 (see indications in Figure 8). The analysis of the deformations in these micropiles and the evolution of the forces inside the steel bars (deduced with the help of the Fellenius method) highlight the progressive buckling of these steel bars. An unloading procedure was thus applied for the two SLT's performed on micropiles ID 1 and 4.

The geotechnical bearing capacity of the different resin grouted micropiles are thus, in the given soil conditions, larger than their structural resistance. Considering the limited settlements measured for all the SLT's (see Figure 8), extrapolation methods (e.g. the Chin method) do not allow to provide reliable values of the geotechnical bearing capacity of the different micropiles.

6 REALIZATION OF A SECOND TEST CAMPAIGN WITH STATIC TENSILE LOAD TESTS

In July 2018, the company GCP APPLIED TECHNOLOGIES has made a second appeal to the Belgian Building Research Institute (BBRI) in order to perform three geotechnical static tension load tests on three isolated resin grouted micropiles. The purpose of this second in-situ test campaign was to determine the uplift resistance of the three different types of resin grouted micropiles when subjected to tensile loads.

The tensile load tests were conducted in September 2018 on the micropiles ID 1, 6 and 4 previously installed on the test site of the BBRI (cf. Section 4 of the present paper).

The resin grouted micropile ID 6 was not subjected to a load test during the first test campaign (cf. Section 5). Nevertheless, the head of this micropile was excavated up to a depth of about 80 cm. This partial excavation was performed in order to have a first idea of the dimensions and the shape of the resin grouted micropile body. If the friction resistance developing along the shaft of the micropile is probably limited in the first meter, it has to be noted that this partial excavation could influence the friction forces measured for this segment (up to 0.8 m depth) during the static tension load test.

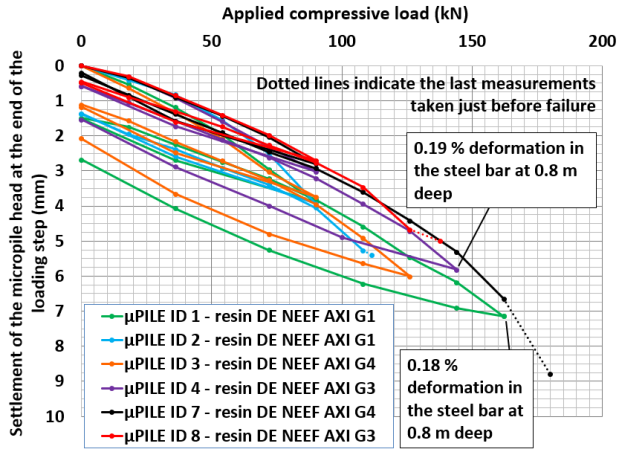

Figure 8. Results of the six static compression load tests performed on the resin grouted micropiles - Settlement at the end of the loading step as a function of the applied load (Denies et al. 2019)

During the first test campaign (cf. Section 5), the micropiles ID 1 and ID 4 were subjected to a static compression load test. For these micropiles, no structural failure happened but a level of deformation close to the yield strength of the steel bar was still observed (see indications in Figure 8) and an unloading procedure was applied. It is thus important to note that the prior realization of these two static compression load tests could influence the results of the tensile tests. The friction resistance of these two micropiles has already been mobilized during the static compression load tests.

As illustrated in Figures 9 and 10, the reaction device for the static tension load tests consists in the assembly of two reaction steel beams installed above the head of the test micropile. These reaction beams are settled on two wood assemblies made of wood beams. The wood assemblies allow the transmission of the reaction force into the ground at a safe distance from the test micropile. For this reaction system, the distance between the center of the test micropile and the nearest edge of each wood assemblies is larger than 2.5 m.

The three static tension load tests were performed according to the NF P 94-150-2 considering one loading cycle and without intermediate unloading cycle. The day of the test, ten constant loading steps of 25 kN (duration of 60 minutes) are applied until the uplift resistance is reached or until a maximal load of 250 kN (larger than the yield strength of the steel bar).

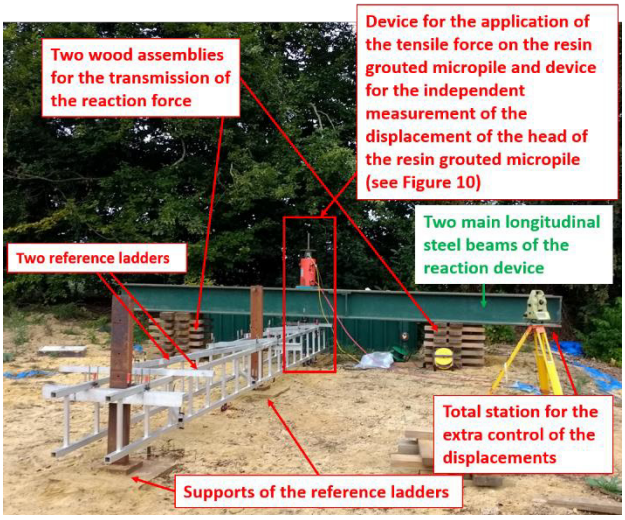

Figure 9. Reaction device and test set-up for the realization of the geotechnical static tension load tests on the resin grouted micropiles

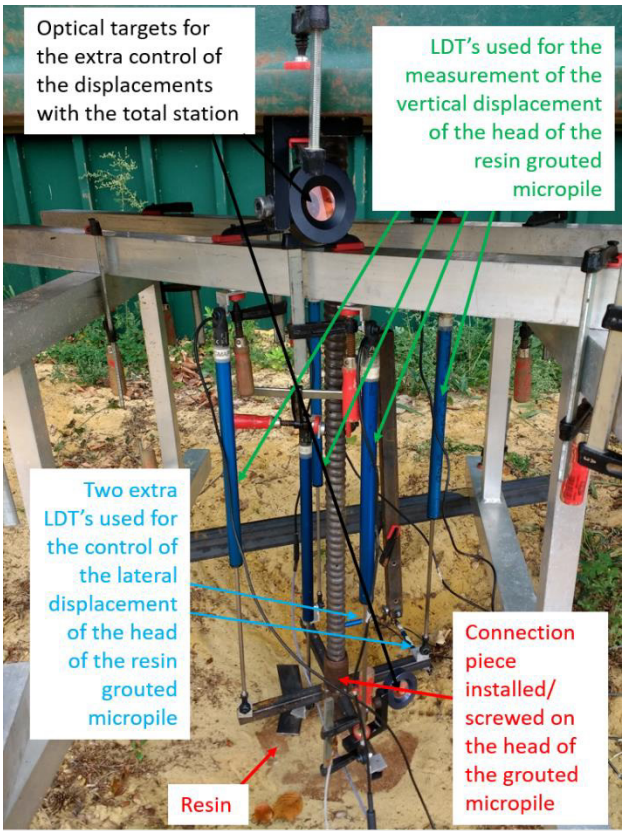

Figure 10. Device for the application of the tensile force on the resin grouted micropile and device for the independent measurement of the displacement of the head of the resin grouted micropile

A comparison of the load-displacement curves of the three tested micropiles is given in Figure 11.

For the micropile ID 1 (resin DE NEEF® AXI G1), the creep behavior was limited until a load of 175 kN. The creep seems to emerge at 200 kN. At 225 kN, the creep is clearly visible. The upward head displacement obtained at the end of the ninth step at 225 kN (i.e. after 60 minutes) was equal to 31.62 mm. At the end of this step, the tensile load was increased until a load of 239 kN was reached. At this moment it was no more possible to increase the load due to the yielding behavior of the steel bar (deformation larger than 8000 µstrain was measured in the steel bar). Nevertheless, considering the evolution of the displacement of the micropile base during the test (see Figure 12), the micropile was not far from its geotechnical ultimate uplift resistance. Defined in agreement with the NF P 94-150-2, the critical creep load obtained for the tensile test performed on the micropile ID 1 was equal to 190 kN and the tensile load at failure was close to 200 kN.

For the micropile ID 6 (resin DE NEEF® AXI G4), the creep behavior was limited until a load of 125 kN was applied. The creep seems to emerge at 150 kN. At 175 kN, the creep is clearly visible. The upward head displacement obtained at the end of the seventh step at 175 kN (i.e. after 60 minutes) was equal to 20.41 mm. At the end of this step, the tensile load was increased until a load of 193 kN was reached. At this moment, there was a sudden failure of the micropile resulting in an abrupt decrease of the load. In spite of two attempts of reload, it was no more possible to maintain a consequent tensile load and the micropile was fully unloaded. As no structural failure of the steel bar was observed at the end of the test (in spite of the level of deformation measured during the test), one can assume that the ultimate uplift resistance of the micropile has been reached during the test. The evolution of the displacement of the micropile base during the test supports this conclusion (see Figure 12).

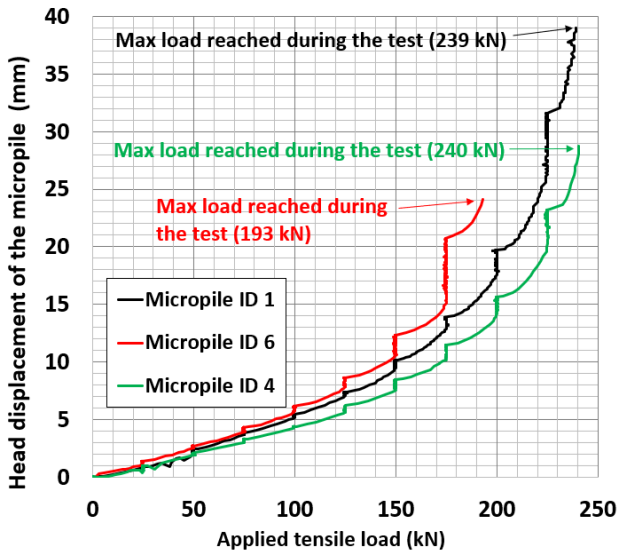

Figure 11. Load-displacement curves for the three static tension load tests performed on the three isolated resin grouted micropile

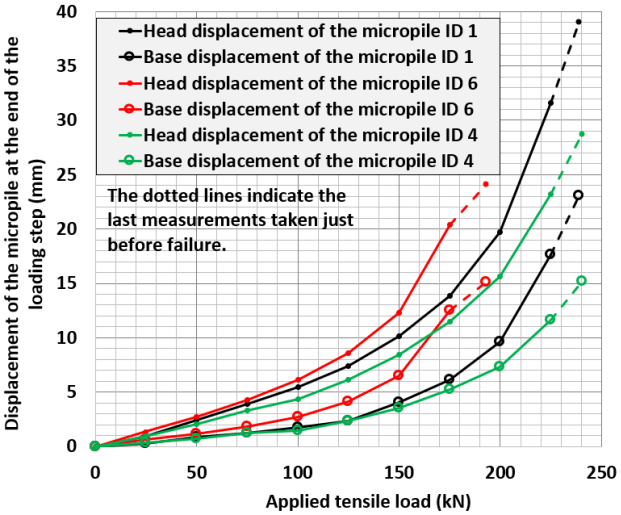

Figure 12. Displacement of the micropile at the end of the loading step as a function of the applied tensile load for the three tested micropiles

Defined in agreement with the NF P 94-150-2, the critical creep load obtained for the tensile test performed on the micropile ID 6 was equal to 140 kN and the tensile load at failure was close to 175 kN.

For the micropile ID 4 (resin DE NEEF® AXI G3), the creep behavior was limited during the test. The micropile starts slowly to creep at 175 kN. The creep is more visible at 225 kN. The upward head displacement obtained at the end of the ninth step at 225 kN (i.e. after 60 minutes) was equal to 23.20 mm. At the end of this step, the tensile load was increased until a load of 240 kN was reached. During the load increase to the last loading step, a structural failure of the steel bar was observed at 240 kN (above the soil surface, in the neighborhood of the coupling sleeve). At that moment, the deformation level measured in the first segment of the bar (at 0.8 m depth) was close to 8000 µstrain. Due to this structural limit, the test was stopped. Nevertheless, considering the evolution of the displacement of the micropile base during the test (see Figure 12), the micropile was not far from its geotechnical ultimate uplift resistance. Defined in agreement with the NF P 94-150-2, the critical creep load obtained for the tensile test performed on the micropile ID 4 was equal to 200 kN and the tensile load at failure was close to 215 kN.

7 EXCAVATION OF THE EIGHT RESIN GROUTED MICROPILES

Finally, after the tests, in order to determine their shape and to study their material properties, the eight resin grouted micropiles were excavated in November 2018. Their perimeter (as a function of the depth) and their total volume were measured with the help of 3D digitization/scanning techniques. It seems that the significant bearing and tensile resistances of the resin grouted micropiles, as observed during the present test campaigns, are, at least partially, related to their particular and irregular shape, as formed in the sand during the injection process (see Figure 13).

8 CONCLUSIONS

During the first test campaign with compressive tests, the geotechnical bearing capacity of the resin grouted micropiles was never reached. Either a structural failure of the steel bar was observed (by buckling) or a high level of deformation was reached in the steel bar. That means that, in the given soil conditions, the bearing capacity of such micropiles is limited by the steel strength, which is very positive for the micropile concept, as the steel strength can be adapted by the customer in function of the design requirements. The result, detailed in Denies et al. (2019), also demonstrate the effective geotechnical behavior of the resin body of the micropile with a significant level of friction mobilization at the interface resin-soil.

During the second test campaign, three static tension load tests were performed on three different isolated resin grouted micropiles. For the tests conducted on micropiles ID 1 and 4, in spite of the fact that these two micropiles had already been tested in compression (cf. Figure 8), they still developed a significant uplift resistance with respective critical creep loads of 190 kN (ID 1) and 200 kN (ID 4) and tensile loads at failure of 200 kN (ID 1) and 215 kN (ID 4). For these two micropiles, the tests were stopped due to the yielding behavior or due to the structural failure of the steel bar. For the micropile ID 6, the uplift resistance was reached with a critical creep load of 140 kN and a tensile load at failure of 175 kN.

After testing, the eight micropiles were excavated to determine their dimensions with the help of 3D digitization/scanning methods. For each micropile, the volume determined by these ways, can be compared to the injected volume of resin.

In addition, a laboratory test campaign on real-scale samples taken from the resin grouted micropiles has been performed to obtain the characteristics of the hardened sand-resin material as produced in-situ. These results will later be published.

9 REFERENCES

AFNOR. NF P 94-105. April 2012. Inspection of compaction quality - Method using a variable energy dynamic penetrometer [in French].

AFNOR. NF P 94-150-1. December 1999. Static test on single pile – Part 1: in compression [in French].

AFNOR. NF P 94-150-2. December 1999. Static test on single pile — Part 2: Tension pile [in French].

Chin, F. K. 1970. Estimation of the Ultimate Load of Piles from Tests Not Carried to Failure. *Proc. of the 2nd Southeast Asian Conf. on Soil Engineering, Singapore City, June 11-15*: 81-92.

Denies, N., Huybrechts, N., de Ruijter, M., Kempenaers, P., Lopes, P. and Smits, D. 2019. In-situ test campaign on innovative resin grouted micropiles. *Proc. of the 17th ECSMGE, Reykjavik, 1-6 September 2019,* doi: 10.32075/17ECSMGE-2019-0145

Fellenius, B. 2001. From strain measurements to load in an instrumented pile. *Geotechnical Instrumentation News*: 35-38.

Huybrechts, N., De Vos, M. and Van Lysebetten, G. 2016. Advances and innovations in measurement techniques and quality control tools. *Proc. of the ISSMGE - ETC 3 Int. Symp. on Design of Piles in Europe. Leuven, April 28 - 29*, Vol. 1, 209-233

ISSMGE TC16. 1999. International Reference Test Procedure for the Cone Penetration Test (CPT) and the Cone Penetration Test with pore pressure (CPTU), Proc. of the 12th ECSMGE, Amsterdam, June 7-10, Vol III: 2195-2222.

Vanden Berghe, J.-F. 2001. Sand strength degradation within the framework of vibratory pile driving. PhD Thesis, UCL.

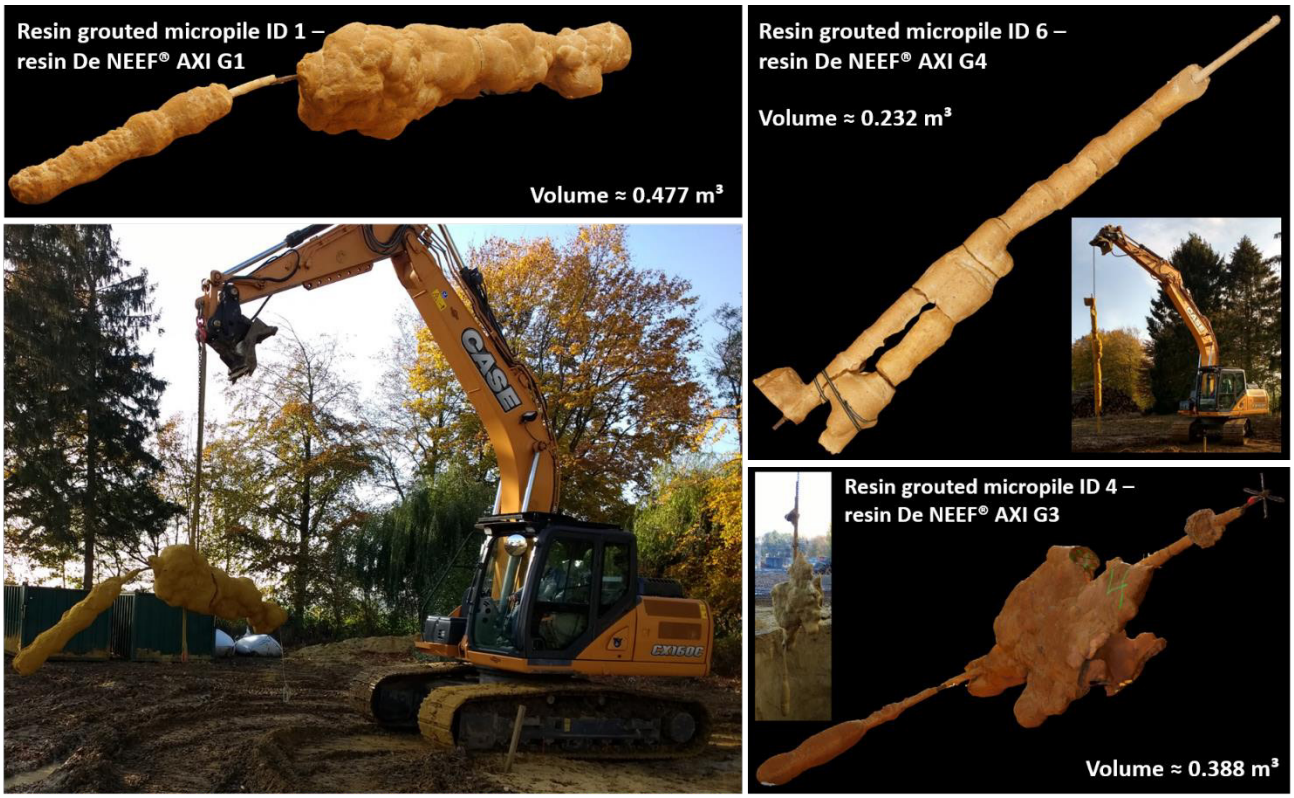

Figure 13. Excavation and 3D digitization/scanning of the resin grouted micropiles ID 1, 4 and 6, after realization of the static tension load tests